Supplement of SOIL, 2, 615–629, 2016
http://www.soil-journal.net/2/615/2016/
doi:10.5194/soil-2-615-2016-supplement

Supplement of

Deriving pedotransfer functions for soil quartz fraction in southern France from reverse modeling

Jean-Christophe Calvet et al.

Correspondence to: Jean-Christophe Calvet (jean-christophe.calvet@meteo.fr)

Supplement # 1

Soil characteristics of the 21 SMOSMANIA stations

Table S1.1 – Soil characteristics at –0.10 m for the 21 stations of the SMOSMANIA network: difference in dry density between soil layers at –0.05 m and –0.10 m ($\Delta\rho_d$), gravimetric fraction of mineral fine earth (*Mn*) of sand, clay, and silt, gravimetric fraction of fine earth (*M*) of soil organic matter (SOM), gravimetric fraction of gravel (m_{gravel}), C/N ratio, and total nitrogen (N_T). The stations are listed from West to East (from top to bottom).

Station (full name)	$\Delta\rho_d$ (kg m^{-3})	Mn_{sand} (%)	Mn_{clay} (%)	Mn_{silt} (%)	M_{SOM} (%)	m_{gravel} (%)	*C/N* (-)	N_T (g kg^{-1})
SBR (Sabres)	–220	93.7	4.2	2.1	2.46	0.27	21.4	0.67
URG (Urgons)	0	15.4	15.8	68.8	2.42	0.93	10.5	1.33
CRD (Créon d'Armagnac)	–130	88.4	5.3	6.3	4.08	0.00	16.0	1.48
PRG (Peyrusse Grande)	–191	15.6	42.3	42.1	4.05	38.51	12.0	1.96
CDM (Condom)	–103	13.4	44.2	42.4	2.61	2.04	11.3	1.34
LHS (Lahas)	18	20.7	41.0	38.3	3.76	9.11	11.5	1.89
SVN (Savenès)	–28	33.9	19.3	46.8	2.15	29.62	11.9	1.04
MNT (Montaut)	–39	31.3	15.3	53.4	2.22	18.81	12.0	1.07
SFL (Saint-Félix-de-Lauragais)	42	40.3	22.4	37.3	3.12	43.36	11.1	1.62
MTM (Mouthoumet)	–102	41.1	30.5	28.4	5.54	51.23	11.0	2.90
LZC (Lézignan- Corbières)	–115	49.0	25.1	25.9	2.76	51.93	10.5	1.53
NBN (Narbonne)	–285	23.2	49.2	27.6	5.97	49.92	12.0	2.89
PZN (Pézenas)	–73	51.9	17.4	39.7	2.56	11.06	13.1	1.13
PRD (Prades-le-Lez)	41	23.7	32.8	43.5	6.04	65.90	13.0	2.69
LGC (La-Grand-Combe)	40	74.8	12.9	12.3	2.73	38.04	22.5	0.70
MZN (Mazan-L'Abbaye)	–143	72.0	12.6	15.4	7.47	23.42	12.2	3.54
VLV (Villevieille)	–158	67.8	12.4	19.8	3.20	6.41	12.2	1.52
BRN (Barnas)	–203	80.4	7.1	12.5	5.61	77.40	16.8	1.93
MJN (Méjannes-le-Clap)	0	42.8	19.3	37.9	8.46	66.11	15.0	3.25
BRZ (Berzème)	–186	34.6	26.4	39.0	3.41	39.59	11.8	1.67
CBR (Cabrières-D'Avignon)	–10	48.8	23.3	27.9	2.58	48.94	10.5	1.42

The gravimetric fractions of sand, clay, and silt (denoted by *x*) are calculated as:

$$m_x = Mn_x \times (1 - M_{SOM}) \times (1 - m_{gravel}) \tag{S1.1}$$

The gravimetric fraction of SOM is calculated as:

$$m_{SOM} = M_{SOM} \times (1 - m_{gravel}) \tag{S1.2}$$

Figure S1.1 presents the Mn_x values at –0.10 m together with values at –0.05 m and –0.20 m, and shows that soil texture does not vary much with depth at a given station.

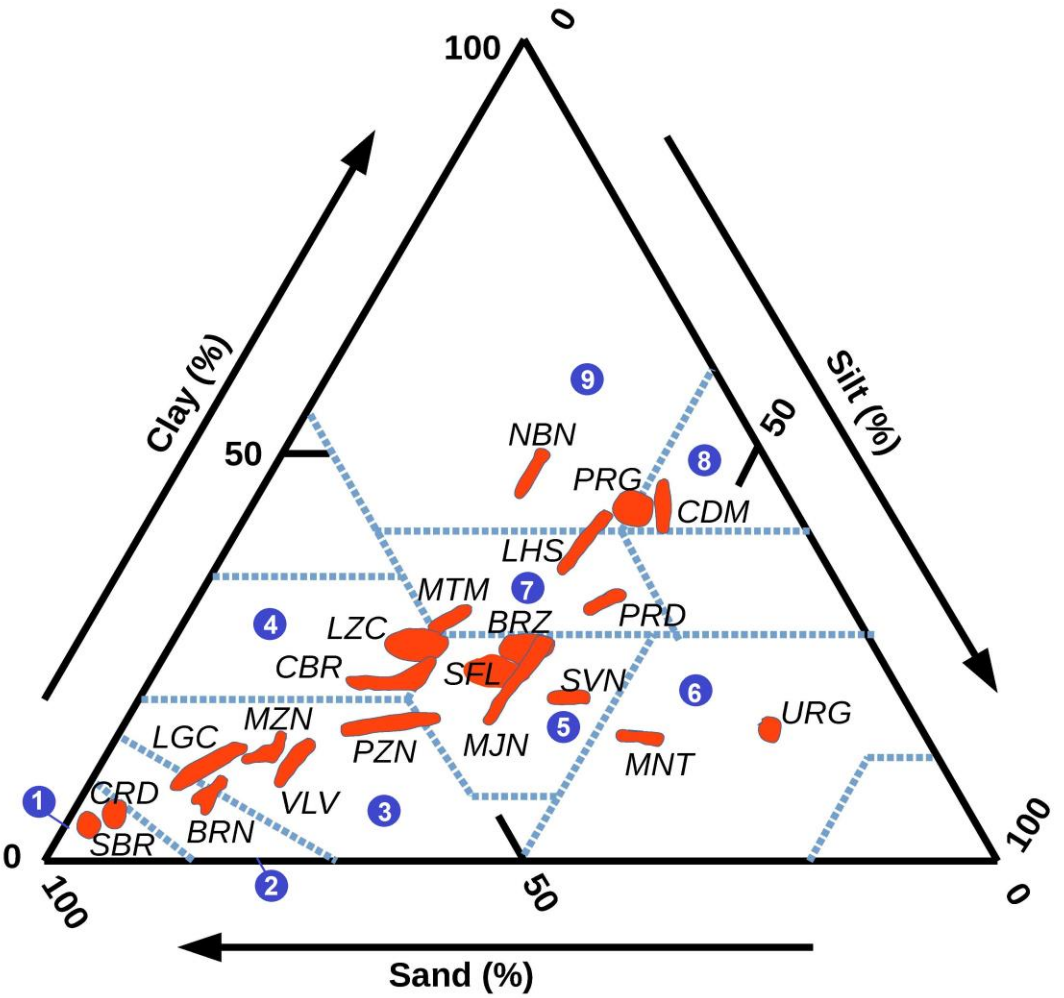

Figure S1.1 – Soil characteristics of the 21 SMOSMANIA stations: mineral fine earth gravimetric fractions of clay, silt and sand. For a given soil, the red mark covers the fraction values measured at 0.05, 0.10 and 0.20 m. Full station names are given in Table S1.1. The dashed blue lines correspond to the USDA textural soil classes:
(1) sand, (2) loamy sand, (3) sandy loam, (4) sandy clay loam, (5) loam, (6) silt loam,
(7) clay loam, (8) silty clay, (9) clay.

Table S1.1 shows that some soils present a very high gravimetric fraction of gravels (up to 77 % for BRN). However, we had no difficulty in measuring soil temperature and soil moisture, including at the BRN site, as shown by Fig. S1.2. Note that the sensors we use are designed to work in such difficult conditions. The ThetaProbe and PT100 sensors have very strong rods, 0.06 m and 0.10 m long, respectively.

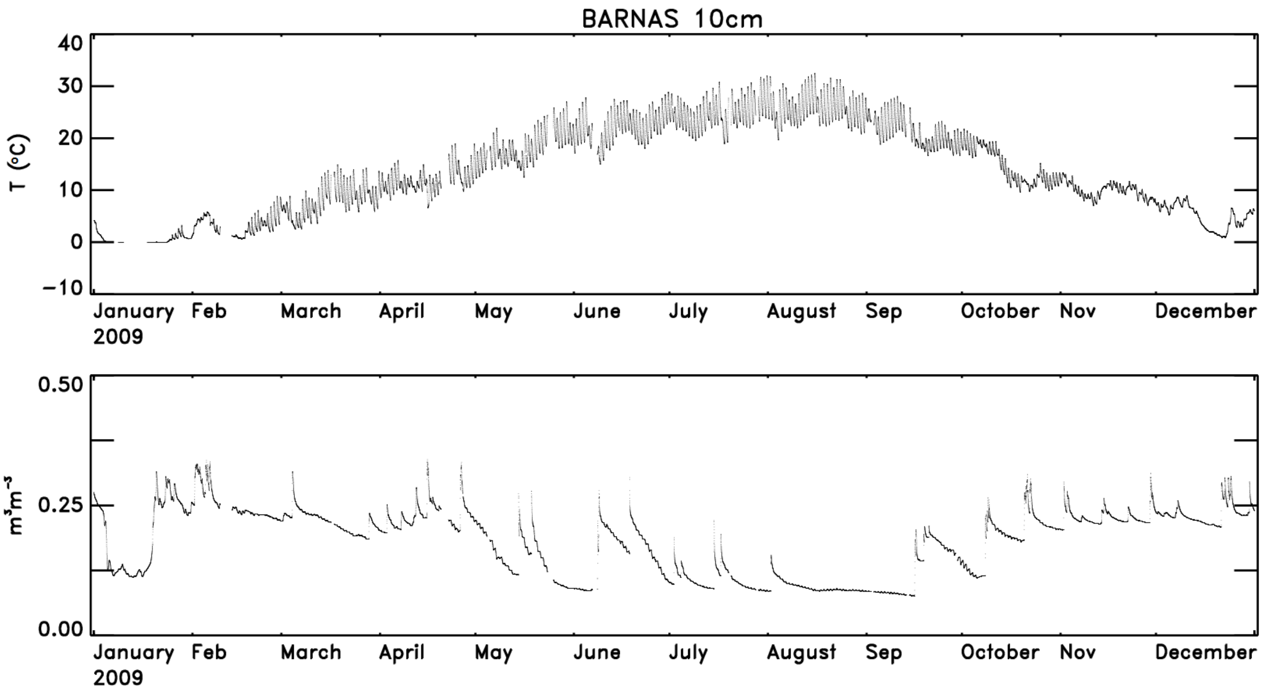

Figure S1.2 - Soil temperature (top) and volumetric soil moisture (bottom) measured in 2009 at the Barnas station (BRN) at a depth of –0.10 m.

The ThetaProbe sensors provide a voltage signal S_V in units of V. In order to convert the voltage signal into volumetric soil moisture content θ (m^3m^{-3}), soil-specific logistic calibration curves were developed using in situ gravimetric soil samples for all stations, and for all depths (z):

$$\theta(z) = K/\left\{1 + a(z)e^{-R(z)\times S_V(z)}\right\} \quad \text{(S1.3)}$$

Values of K, a(z), and R(z) coefficients are given in Table S1.2.

Table S1.2 – Soil-specific coefficients of a logistic calibration curve (Eq. S1.3) for the 21 stations of the SMOSMANIA network. The stations are listed from West to East (from top to bottom).

Station	*K* (m^3m^{-3})	*R*@-5cm (V^{-1})	*R*@-10cm (V^{-1})	*R*@-20cm (V^{-1})	*R*@-30cm (V^{-1})	*a*@-5cm (–)	*a*@-10cm (–)	*a*@-20cm (–)	*a*@-30cm (–)
SBR	0.35	6.546	5.009	6.752	3.052	17.89	15.66	33.02	7.11
URG	0.60	4.558	3.932	4.597	4.234	19.99	19.16	38.44	31.00
CRD	0.44	6.065	3.930	4.620	4.079	13.57	13.36	17.62	18.19
PRG	0.60	3.773	4.530	5.270	4.511	19.89	35.91	70.25	35.52
CDM	0.60	4.198	3.968	8.511	9.628	24.73	18.97	959.10	2713.51
LHS	0.60	4.719	3.766	4.539	7.336	27.61	19.65	35.73	558.92
SVN	0.60	3.627	2.569	2.882	3.019	14.86	11.03	13.53	18.01
MNT	0.60	3.869	3.098	3.605	2.877	11.60	11.02	20.43	12.30
SFL	0.60	3.442	2.926	4.022	4.459	18.54	9.38	24.51	31.41
MTM	0.60	2.377	3.130	2.264	2.888	8.26	10.62	6.01	13.34
LZC	0.60	4.596	4.241	5.030	2.405	35.23	37.83	53.09	19.32
NBN	0.60	3.426	3.702	5.043	7.333	12.58	12.78	37.26	226.11
PZN	0.60	4.410	6.400	3.950	4.758	25.08	58.50	25.89	37.04
PRD	0.60	4.299	4.573	4.449	4.649	26.23	37.11	40.61	47.99
LGC	0.43	5.037	4.723	5.676	7.163	20.37	15.77	38.59	134.96
MZN	0.60	4.770	5.726	4.326	5.394	32.30	72.97	24.58	66.15
VLV	0.60	3.879	3.600	5.236	4.887	23.38	17.06	58.85	48.91
BRN	0.38	7.104	5.585	4.002	6.473	13.89	11.99	9.84	17.12
MJN	0.60	4.547	3.496	3.697	4.136	18.50	14.64	15.94	21.71
BRZ	0.60	3.747	3.355	2.678	3.191	14.38	12.24	11.25	13.65
CBR	0.60	6.239	4.600	3.550	3.598	151.11	26.08	24.48	24.68

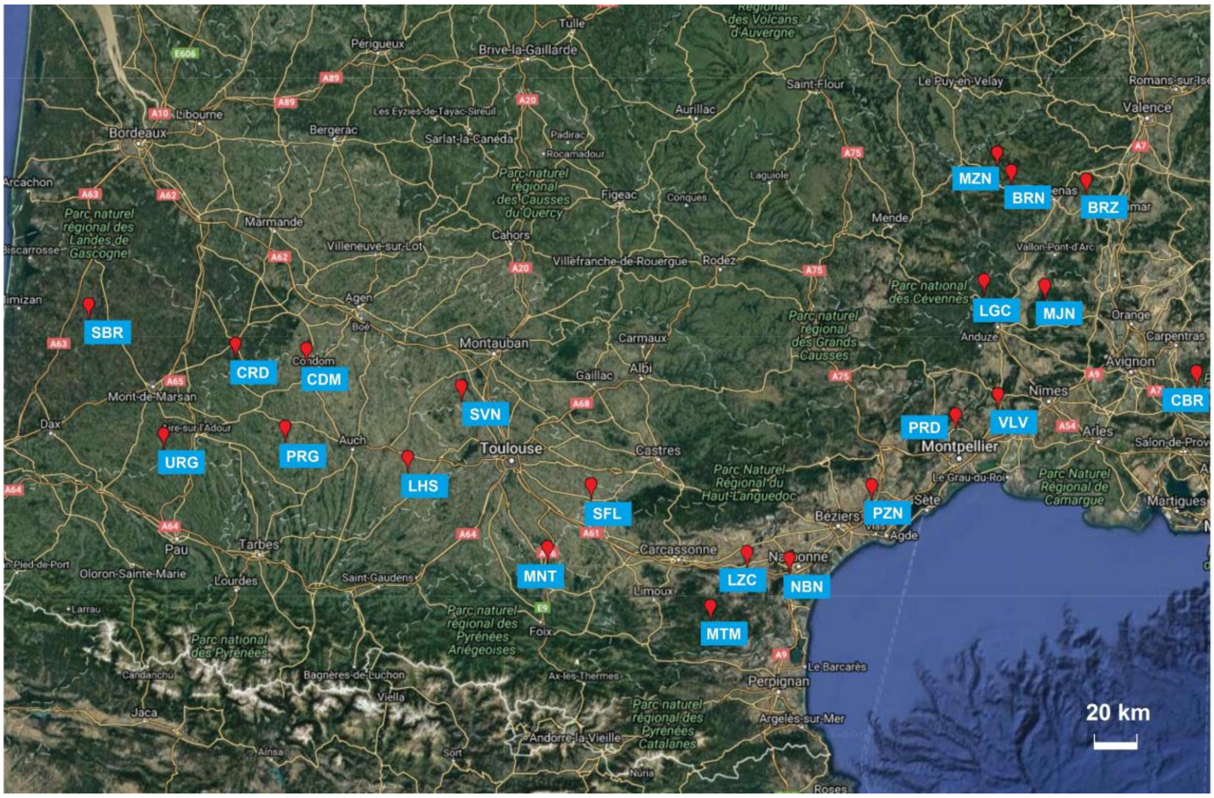

Figure S1.3 - Location of the 21 SMOSMANIA stations in southern France (see station names in Table S1.1). Background geographic information is from Google Maps.

The SMOSMANIA network forms an Atlantic-Mediterranean transect. SBR and CRD are located in agricultural spots in the Les Landes pine forest area, on sandy soils. URG, PRG, CDM, LHS, SVN, MNT and SFL are in the Garonne plain, characterized by croplands and grasslands over undulating terrain. CDM and PRG are on silty clay soil and URG and MNT on silt loams. LZC, NBN, PZN, PRD, VLV, and CBR are in the Mediterranean plain on croplands or mosaics of crops, vineyards, and orchards. Other stations in the Mediterranean area are located in the Corbières, and Cévennes mountainous areas (at altitudes higher than 450 m above sea level) covered by forests or shrubs: MTM, LGC, MZN, BRN, BRZ. MJN is located in a shrub area. The Mediterranean part of the transect is characterized by loamy sands (BRN and LGC), sandy loams (MZN, VLV, PZN), and sandy clay loams (LZC, CBR).

Figure S1.4 - Automatic weather station of Montaut (MNT).

Figure S1.5 - Installation of the probes at Sabres (SBR).

Figure S1.6 - Installation of the probes at Montaut (MNT).

Figure S1.7 - Installation of the probes at Barnas (BRN).

Figure S1.8 - Installation of the probes at Mouthoumet (MTM).

Figure S1.9 - Installation of the probes at Prades-le-Lez (PRD).

Figure S1.10 - Soil sample collection at Prades-le-Lez (PRD).

Supplement # 2

Data filtering technique to limit the impact of soil heterogeneities

The impact of vertical heterogeneities in λ values has to be accounted for in the λ retrieval technique. In order to address this issue, a data analysis procedure aiming at limiting this effect as much as possible was implemented. We used only the soil temperature data presenting a relatively low vertical gradient close to the soil surface, where most differences with deeper layers are found. It must be noted that if this data sorting is omitted, the retrieved λ_{sat} values are lower for all the stations. The procedure is described below.

The 1D Fourier equation in heterogeneous soil conditions can be written as:

$$C_h \frac{\partial T}{\partial t} = \frac{\partial}{\partial z}\left(\lambda \frac{\partial T}{\partial z} \right) \qquad \text{(S2.1)}$$

and discretized as:

$$\frac{T_i^n - T_i^{n-1}}{\Delta t} = \frac{1}{C_{hi}}\left[\frac{1}{2}\left(\frac{\lambda_{i+1/2}\gamma_{i+1}^n - \lambda_{i-1/2}\gamma_i^n}{\Delta z_m} \right) + \frac{1}{2}\left(\frac{\lambda_{i+1/2}\gamma_{i+1}^{n-1} - \lambda_{i-1/2}\gamma_i^{n-1}}{\Delta z_m} \right) \right] \qquad \text{(S2.2)}$$

In this study, we assumed that the retrieved λ values, at a depth of –0.10 m, were representative of a bulk soil layer including the three soil temperature probes used to retrieve the thermal diffusivity, and did not differ much from the interfacial λ values along the bottom and top edges of the considered soil layer ($\lambda_{i+1/2}$ and $\lambda_{i-1/2}$, respectively):

$$\lambda \approx \lambda_{i+1/2} \approx \lambda_{i-1/2} \qquad \text{(S2.3)}$$

and, at a given time *n*,

$$\lambda\gamma_{i+1}^n - \lambda\gamma_i^n \approx \lambda_{i+1/2}\gamma_{i+1}^n - \lambda_{i-1/2}\gamma_i^n \qquad \text{(S2.4).}$$

In reality, differences may occur:

$$\Delta\lambda = \lambda_{i+1/2} - \lambda_{i-1/2} \qquad \text{(S2.5).}$$

Considering the temperature gradient ratio R_{TG} at a given time *n*:

$$R_{TG} = \frac{\gamma_i^n}{\gamma_i^n - \gamma_{i+1}^n} \quad \text{(S2.6)}$$

and combining Eqs. (S2.4), (S2.5) and (S2.6), the retrieved λ can be written as:

$$\lambda \approx \lambda_{i+1/2} - R_{TG}\ \Delta\lambda \quad \text{(S2.7).}$$

Since soil temperature gradients were more pronounced close to the soil surface and since, more often than not, soil density presented smaller values close to the soil surface, the $\Delta\lambda$, R_{TG}, and $R_{TG}\Delta\lambda$ values were ≥ 0. Since in the soils considered in this study, differences in soil density were much less pronounced at depth than between the –0.05m and –0.10m soil layers, we considered that $\lambda_{i+1/2}$ was closer to the final value to be retrieved, λ^*, than the initial λ retrieval:

$$\lambda^* \approx \lambda + R_{TG}\ \Delta\lambda \quad \text{(S2.8).}$$

Eq. (S2.8) shows that the target λ^* value is larger than the initial λ retrieval. The relative error on λ^* can be written as $R_{TG}\Delta\lambda/\lambda^*$ (dimensionless). We used $R_{TG}\Delta\lambda/\lambda^*$ as an indicator of the quality of the λ retrieval, with large values of $R_{TG}\Delta\lambda/\lambda^*$ corresponding to erroneous estimates. In the revised data analysis procedure. The λ retrieval corresponding to high $R_{TG}\Delta\lambda/\lambda^*$ values were excluded from the analysis. The following condition was used:

$$R_{TG}\Delta\lambda/\lambda^* < 10\% \quad \text{(S2.9).}$$

Finally, a subset of 20 λ retrievals per station was used, at most, corresponding to the lowest $R_{TG}\Delta\lambda/\lambda^*$ values.

The NBN, PZN, BRZ, and MJN observations were completely filtered out as they presented $R_{TG}\Delta\lambda/\lambda^*$ values systematically higher than 10%. The impact of the refined data selection is illustrated in Fig. S2.1 for the MNT and LHS soils.

In practise, the $\Delta\lambda$ term was estimated using the $\Delta\rho_d$ values of Table S1.1 and the sensitivity of λ to changes in dry density, $\Delta\lambda/\Delta\rho_d$. The latter was derived numerically using the Eqs. (7)-(13) model, in soil wetness conditions ranging from $S_d = 0.4$ to $S_d = 1$.

Since the derivation of $\Delta\lambda/\Delta\rho_d$ depends on the obtained f_q pedotransfer function, $\Delta\lambda/\Delta\rho_d$ values were recalculated with the new pedotransfer function, and a few iterations permitted refining these estimates.

At saturation ($S_d = 1$) $\Delta\lambda/\Delta\rho_d$ ranged between 0.64×10^{-3} Wm^{2}K^{-1}kg^{-1} for PRD to 1.24×10^{-3} Wm^{2}K^{-1}kg^{-1} for SBR.

At $S_d = 0.4$, $\Delta\lambda/\Delta\rho_d$ ranged between 0.46×10^{-3} Wm^{2}K^{-1}kg^{-1} for PRD to 0.81×10^{-3} Wm^{2}K^{-1}kg^{-1} for SBR.

R_{TG} ranged between 0.5 and 2.4, with a median value of 1.3.

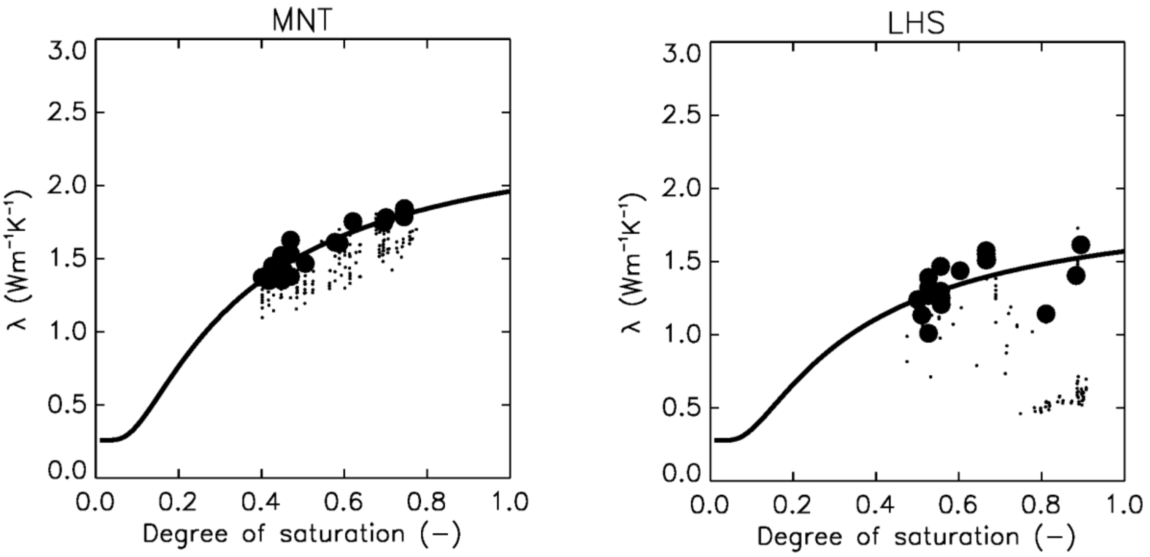

Figure S2.1 - Retrieved and modelled λ values (dots and solid line, respectively) vs. the observed degree of saturation of the soil, at a depth of 0.10 m for the MNT and LHS stations. The 20 λ retrievals used to fit the thermal conductivity model and retrieve λ_{sat} are represented by large dots.

Supplement # 3

Impact of soil volumetric heat capacity of soil solids on the retrieved λ_{sat}

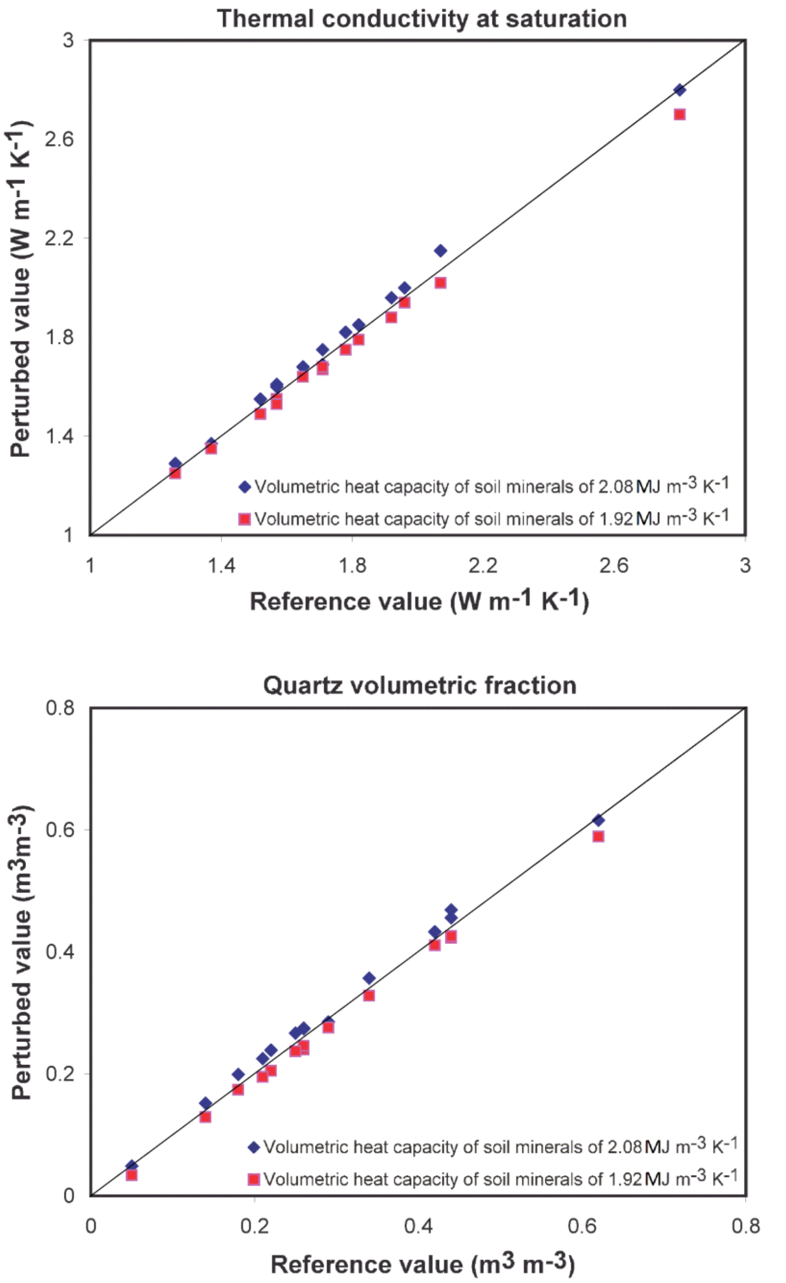

Figure S3.1 – Impact of using values of C_{hmin} = 1.92 MJ m^{-3} K^{-1} and C_{hmin} = 2.08 MJ m^{-3} K^{-1} instead of C_{hmin} = 2.0 MJ m^{-3} K^{-1} on the 14 retrieved values (Table 2) of (top) λ_{sat}, (bottom) volumetric fraction of quartz.

Supplement # 4

Characteristics of 10 Chinese soils

Table S4.1 – Soil characteristics of ten Chinese soils of Lu et al. (2007). ρ_d, θ_{sat}, f, and m, stand for soil bulk density, porosity, volumetric fractions, and gravimetric fractions, respectively. These soils consist of reassembled sieved soil samples and m_{gravel} = 0 kg kg^{-1}. λ_{sat} experimental values are derived from Table 3 in Tarnawski et al. (2009). Soil density is derived from porosity values inverting Eq. (1). The soils are sorted from the largest to the smallest ratio of m_{sand} to m_{SOM}. The ratio values smaller than 40 are in bold.

Lu et al. (2007) soils	λ_{sat} observations (Wm^{-1}K^{-1})	ρ_d (kg m^{-3})	θ_{sat} (m^{3}m^{-3})	f_{sand} (m^{3}m^{-3})	f_{clay} (m^{3}m^{-3})	f_{silt} (m^{3}m^{-3})	f_{SOM} (m^{3}m^{-3})	m_{sand} (kg kg^{-1})	m_{clay} (kg kg^{-1})	m_{silt} (kg kg^{-1})	m_{SOM} (kg kg^{-1})	$\frac{m_{sand}}{m_{SOM}}$
Sand 2	1.87	1567	0.41	0.548	0.035	0.006	0.001	0.929	0.060	0.010	0.001	1327.6
Sand 1	2.19	1567	0.41	0.553	0.029	0.006	0.001	0.939	0.050	0.010	0.001	1043.5
Loam 11	1.62	1350	0.49	0.253	0.046	0.208	0.003	0.499	0.090	0.409	0.003	199.5
Clay loam 9	1.36	1270	0.52	0.152	0.143	0.181	0.003	0.319	0.299	0.379	0.003	118.2
Sandy loam 3	1.68	1333	0.49	0.333	0.060	0.104	0.009	0.664	0.119	0.208	0.009	77.2
Loam 4	1.40	1264	0.52	0.189	0.052	0.232	0.005	0.398	0.109	0.488	0.005	81.2
Silty clay loam 7	1.34	1267	0.52	0.090	0.128	0.256	0.004	0.189	0.269	0.538	0.004	48.5
Silt loam 5	1.38	1272	0.51	0.128	0.104	0.241	0.012	0.267	0.217	0.504	0.012	**22.4**
Silt loam 6	1.47	1255	0.52	0.051	0.089	0.328	0.008	0.109	0.188	0.694	0.008	**13.0**
Silty clay loam 8	1.31	1202	0.52	0.035	0.140	0.263	0.028	0.078	0.310	0.582	0.030	**2.6**

References:

Lu, S., Ren, T., Gong, Y., and Horton, R.: An improved model for predicting soil thermal conductivity from water content at room temperature, Soil Sci. Soc. Am. J., 71, 8–14, doi:10.2136/sssaj2006.0041, 2007.

Tarnawski, V. R., Momose, T., and Leong, W. H.: Assessing the impact of quartz content on the prediction of soil thermal conductivity, Géotechnique, 59, 4, 331–338, doi: 10.1680/geot.2009.59.4.331, 2009.

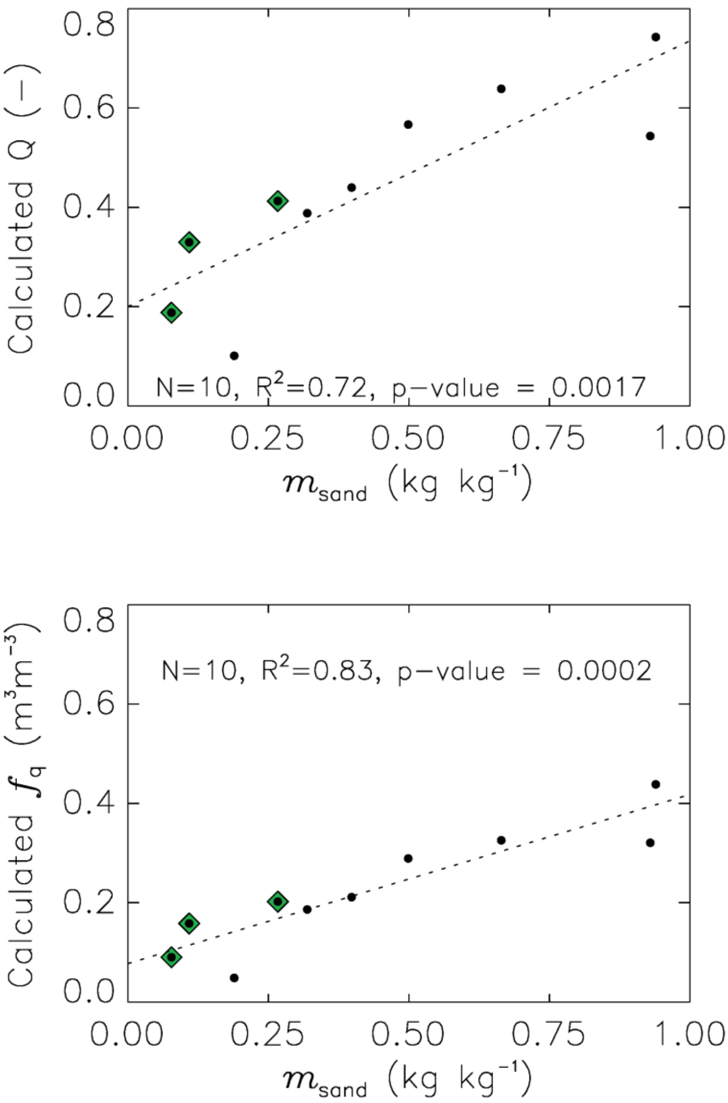

Figure S4.1 – Gravimetric and volumetric fraction of quartz (top and bottom, respectively) derived by Tarnawski et al. (2009) from the λ_{sat} observations of Lu et al. (2007) for 10 soils , vs. the gravimetric fraction of sand m_{sand}. The three soils for which $m_{sand}/m_{SOM} < 40$ are indicated by green diamonds. The dashed lines represent the regression equations based on all soils: $Q = 0.20 + 0.54\ m_{sand}$ and $f_q = 0.08 + 0.34\ m_{sand}$.

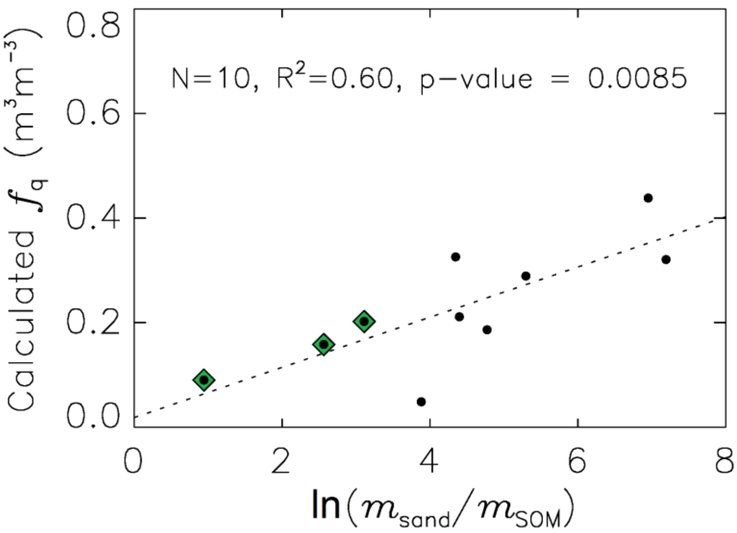

Figure S4.2 – Volumetric fraction of quartz derived by Tarnawski et al. (2009) from the λ_{sat} observations of Lu et al. (2007), vs. the logarithm of the m_{sand} / m_{SOM} ratio. The three soils for which m_{sand}/m_{SOM} < 40 are indicated by green diamonds. The dashed line represents the regression equation: $f_q = 0.02 + 0.048 \ln(m_{sand}/m_{SOM})$.

Supplement # 5

Data filtering to limit the impact of low resolution soil temperature

Since T_i is recorded with a resolution of

$$\Delta T_i = \left|\partial\left(T_i^n - T_i^{n-1}\right)\right| = \left|\partial\left(T_{i+1}^n - T_i^n\right)\right| = 0.1°C \qquad \text{(S5.1)},$$

the retrieved D_h values are affected by uncertainties and the relative uncertainty of D_h can be estimated as:

$$\left|\frac{\partial D_{hi}}{D_{hi}}\right| = \Delta T_i \times \left\{\frac{1}{\left|T_i^n - T_i^{n-1}\right|} + \frac{\Delta z_{i+1}^{-1} + \Delta z_i^{-1}}{\left|\gamma_{i+1}^n - \gamma_i^n\right| + \left|\gamma_{i+1}^{n-1} - \gamma_i^{n-1}\right|}\right\} \qquad \text{(S5.2)}.$$

Therefore, D_h retrievals are more accurate in conditions when soil temperature at z_i = –0.10 m changes rapidly and when differences in vertical gradients of soil temperature above and below z_i are more pronounced. In general, this occurs around noon (between 0900 LST and 1400 LST), and at dusk to a lesser extent, between 1700 LST and 0000 LST. In this study, we have imposed the following conditions for using the obtained D_h retrievals:

$$\left|T_i^n - T_i^{n-1}\right| > 0.8°C\,,\ \left|\gamma_{i+1}^n - \gamma_i^n\right| > 30Km^{-1}\text{, and } \left|\gamma_{i+1}^{n-1} - \gamma_i^{n-1}\right| > 30Km^{-1} \qquad \text{(S5.3)}.$$

According to Eqs. (S5.1)-(S5.2), this ensures that

$$\left|\frac{\partial D_{hi}}{D_{hi}}\right| < 18\% \qquad \text{(S5.4)}.$$